Elsevier Editorial System(tm) for Journal of Alloys and Compounds

Manuscript Draft

Manuscript Number:

Title: Thermal and corrosion behavior of as cast Al-Si alloys with rare earth elements

Article Type: Full Length Article

Keywords: Al-Si alloys, rare earth elements, as cast conditions, microstructure, corrosion, differential thermal analysis

Corresponding Author: Dr. Elisa Canepa,

Corresponding Author's Institution: CNR-ISMAR

First Author: Anna M Cardinale

Order of Authors: Anna M Cardinale; Daniele Macciò; Giorgio Luciano; Elisa Canepa; Pierluigi Traverso

Abstract: Aluminum silicon based alloys are the most important commercial casting alloys. Their cast microstructure is strongly related to their technical properties. By adding other selected alloying elements, the alloy microstructure is known to be modified, thus improving its desired properties. Rare earths (RE) can be used as alloying elements to achieve better technical performance of Al-Si based alloys.
In this work, the effects of individual RE (La, Pr, Nd, Sm, Gd, Tb, Dy or Er) addition on a hypoeutectic as cast Al-Si alloy were studied. In order to investigate the correlation between microstructure changes and thermal and corrosion behavior, the microstructure of the samples and of the intermetallic phases was examined by scanning electron microscopy, electron microprobe analysis, and X-ray powder diffraction. Differential thermal analysis was performed to determine ternary eutectic reaction temperature. A similar decrease in eutectic temperature was recorded for all Al-Si-RE samples. Decreased hardness due to RE addition was shown by Vickers hardness measurements. DC polarization potentiodynamic measurements showed that RE addition increased corrosion resistance in 3.5 wt.% NaCl solution.

Corresponding author:

Elisa Canepa
CNR-ISMAR
Via De Marini 6
I-16149 Genova, Italy
Tel. + 39 010 6475 403
Fax + 39 010 6475 400
E-mail: elisa.canepa@ismar.cnr.it
http://www.ismar.cnr.it/index_html

15/03/2016

Dear Dr. Greneche,

We are submitting a totally revised version of JALCOM-D-14-03966 (you informed us about the non-acceptance decision on 20 Jun 2014).

Following the suggestions of the referees, we have made deep conceptual changes to the manuscript, the text has been edited for English language, the title has been changed accordingly to new contents, and the authorship has been modified by the addition of myself.

We would greatly appreciate your consideration of:
Full length article
"Thermal and corrosion behavior of as cast Al-Si alloys with rare earth elements"
by Anna Maria Cardinale, Daniele Macciò, Giorgio Luciano, Elisa Canepa, Pierluigi Traverso

Best regards,
Elisa Canepa

Prime Novelty Statement

We confirm that:

1) this manuscript is the original work of the authors and has not been published nor has it been submitted simultaneously elsewhere;
2) all the authors have checked the manuscript and have agreed to the submission.

15/03/2016

Corresponding author:

Elisa Canepa
CNR-ISMAR
Via De Marini 6
I-16149 Genova, Italy
Tel. + 39 010 6475 403
Fax + 39 010 6475 400
E-mail: elisa.canepa@ismar.cnr.it
http://www.ismar.cnr.it/index_html

Thermal and corrosion behavior of as cast Al-Si alloys with rare earth elements

Anna Maria Cardinale[a], Daniele Macciò[b], Giorgio Luciano[c1], Elisa Canepa[d*], Pierluigi Traverso[e]

[a] Dipartimento di Chimica e Chimica Industriale, Università di Genova, Via Dodecaneso 31, 16146 Genova, Italy, cardinal@chimica.unige.it,

[b] Dipartimento di Chimica e Chimica Industriale, Università di Genova, Via Dodecaneso 31, 16146 Genova, Italy, maccio@chimica.unige.it

[c] ISMAR-CNR, U.O.S. di Genova, Via de Marini 6-Torre di Francia, 16149 Genova, Italy, giorgio.luciano@ge.ismar.cnr.it

[d] ISMAR-CNR, U.O.S. di Genova, Via de Marini 6-Torre di Francia, 16149 Genova, Italy, elisa.canepa@ismar.cnr.it, [*]Corresponding author

[e] ISMAR-CNR, U.O.S. di Genova, Via de Marini 6-Torre di Francia, 16149 Genova, Italy, pierluigi.traverso@ismar.cnr.it

Key words: Al-Si alloys, rare earth elements, as cast conditions, microstructure, corrosion, differential thermal analysis

Highlights

- Effects of different RE addition on a hypoeutectic as cast Al-Si alloy are studied
- EDX, XRD, and DTA analyses of Al-Si-RE samples are carried out
- Decrease in eutectic temperature is similar for all Al-Si-RE samples
- Decrease in Vickers hardness is similar for all Al-Si-RE samples
- RE addition increases corrosion resistance in 3.5 wt.% NaCl solution

Abstract

Aluminum silicon based alloys are the most important commercial casting alloys. Their cast microstructure is strongly related to their technical properties. By adding other selected alloying elements, the alloy microstructure is known to be modified, thus improving its desired properties. Rare earths (RE) can be used as alloying elements to achieve better technical performance of Al-Si based alloys.

[1] Present address: ISMAC-CNR, U.O.S. di Genova, Via de Marini 6-Torre di Francia, 16149 Genova, Italy

In this work, the effects of individual RE (La, Pr, Nd, Sm, Gd, Tb, Dy or Er) addition on a hypoeutectic as cast Al-Si alloy were studied. In order to investigate the correlation between microstructure changes and thermal and corrosion behavior, the microstructure of the samples and of the intermetallic phases was examined by scanning electron microscopy, electron microprobe analysis, and X-ray powder diffraction. Differential thermal analysis was performed to determine ternary eutectic reaction temperature. A similar decrease in eutectic temperature was recorded for all Al-Si-RE samples. Decreased hardness due to RE addition was shown by Vickers hardness measurements. DC polarization potentiodynamic measurements showed that RE addition increased corrosion resistance in 3.5 wt.% NaCl solution.

1. Introduction

Al-Si alloys are important and widely used casting alloys for their excellent properties, such as low density, low thermal expansion coefficient, good casting performance, good weldability, high wear resistance, good corrosion resistance, and high temperature strength [1,2]. In particular, such properties are very attractive to the transport industry – from aerospace to the automotive and naval sector – where better performance and lower environmental impact can be achieved through vehicle weight reduction. The addition of other alloying elements, at a very low concentration, has been commonly reported in the literature to improve some of the above listed properties [3,4]. Nevertheless, corrosion behavior must be carefully evaluated in order to avoid any detrimental effects [5,6].

Different conversion coatings have been used with the aim of improving Al alloys' corrosion resistance and extending their service time, through both localized corrosion reduction and paint adhesion increase. Chromate-based processes have a strong oxidising power, which inhibits corrosion by forming a new, strong, and efficient passive layer on the substrate surface [7-9]. For almost a century, chromate conversion coatings and anodising pre-treatments with chromic acid had been widely and universally employed. However, they are currently banned in many countries due to their toxicity and carcinogenicity [10-12]. Therefore, extensive efforts have been made to develop alternative environment-friendly conversion films, in compliance with the European Community Regulation on chemicals and their safe use (2006). For such purposes, rare earths (RE) have drawn significant attention [13-15].

RE salts have proven to be the most promising Al alloy corrosion inhibitors [5,11,16-20]. Recent studies have shown that RE protective action is closely linked to its power to inhibit the cathodic corrosion process, by decreasing oxygen reduction reaction kinetics [11,21-23]. This inhibition efficiency tends to increase with increasing immersion time [24]. These results were mainly obtained studying a variety of RE conversion solutions, heated or at room temperature, by dip immersion or spray processes.

Direct RE addition into the alloys during the synthesis was mainly studied for Al-Mg, Al-Zn-Mg and Al-Zn-Mg-Cu alloys [e.g., 25-30]. Direct Sc, Yb, Nd, Pr and Er addition modifies the alloy microstructure (e.g., grain refinement, inhibition of recrystallization, etc.) by improving both its mechanical and chemical properties [31-33]. Sc addition remarkably increases the mechanical properties of different Al alloys, without significant loss in corrosion properties [34-37] and, after specific heat treatments, even with increased resistance to stress corrosion cracking. . Small amounts of Sc improve ductility and strength of Al-Mg alloys due to the formation of fine Al_3Sc precipitates which not only refine grains, but also provide some precipitation hardening [38,39]. Moreover, Sc addition also permits superplasticity in Al-Mg alloys [40]. No significant deleterious effects of Sc addition on general corrosion or pitting corrosion behavior of Al-Mg alloys have been reported [35,36]. Unfortunately, the prohibitively high cost of Sc strictly limits its application. Yb - with Zr and Cr - addition to Al-Mg and Al-Zn-Mg-Cu alloys improve the alloy mechanical performance without significant corrosion resistance loss [41,42]. Nd addition to Al-Mg alloys increases alloy hardness without any significant effect on pitting or general corrosion. On the contrary, the extent of intergranular corrosion following sensitization decreases substantially [43]. Pr (with Zr and Cr) and Er (with Zr and Cr) addition to Al-Zn-Mg-Cu alloys after specific heat treatments, increases resistance to intergranular corrosion, exfoliation corrosion, and stress corrosion, while simultaneously improving strength, fracture toughness, and ductility [44,45]. However, to the best of our knowledge, no study about the effects of direct RE addition on corrosion behavior of Al-Si alloys has ever been performed.

Previous studies of direct RE addition to a casting (hypoeutectic or hypereutectic) Al-Si alloy mainly focused on changes of its microstructure inducing a eutectic temperature lowering. Hence, the measure of such decrease has been proposed as a method to verify any alloy microstructure changes by means of thermal analysis measurements [46-48]. As far as Al-Si-RE phase diagrams are concerned, only few and only partially investigated, Al-Si-RE isothermal sections have been reported in the literature (see [49] and the references therein).

Due to the commercial relevance of Al-Si based casting alloys, the purpose of our work was to study the thermal effects of direct individual RE addition (La, Pr, Nd, Sm, Gd, Tb, Dy, or Er) to a hypoeutectic Al-Si alloy in as cast conditions,. Microstructures and crystallography were investigated by scanning electron microscopy (SEM) and electron probe microanalysis based on energy dispersive X-ray spectroscopy (EDX). Differential thermal analysis (DTA) was used to determine the phase transition temperature and eutectic temperature depression.

Furthermore, in this work, we also investigated corrosion inhibition following addition of La, Pr, Sm, or Tb to Al-Si alloys exposed to a chloride corrosive solution. Electrochemical techniques - such us potentiodynamic polarization - and surface analysis - like SEM coupled with EDX - were used in order to provide information on the interaction between RE compounds and the corroding surface.

2. Experimental procedure

2.1 Synthesis of samples

The composition concentration range of industrially relevant Al-Si alloys usually lies near the binary Al-Si eutectic composition concentration, to which the RE mischmetal is usually added. In this work, all Al-Si samples were prepared with direct individual addition of a RE (La, Pr, Nd, Sm, Gd, Tb, Dy or Er) according to the composition reported in Table 1. A hypoeutectic Al-Si alloy was prepared as reference for each measure. The elements used as starting materials were Al 99.999 wt. % nominal purity, Si 99.99 wt. % nominal purity, and RE 99.9 wt. % nominal purity, supplied by NewmetKoch, Waltham Abbey, England.

For each sample, an Al-Si master alloy was prepared. Stoichiometric amounts of the metals were weighed as small pieces that were arc melted under vacuum. The selected RE was then added to the Al-Si sample remelting the sample to obtain the ternary as cast alloy; the weight of each sample was about 3g. Mass loss was less than 0.5 wt.%. Slices were obtained from the bulk sample by cutting it with a precision cut-off machine equipped with an abrasive precision cut-off wheel, suitable for 500-800 Vickers hardness alloys. Small 1–1.5 mm thick discs, were obtained.

2.2 Structure characterization and hardness measurements

The samples were analyzed by scanning electron microscopy (SEM) and electron probe microanalysis based on energy dispersive X-ray spectroscopy (EDX), in order to investigate both microstructure and phase composition. Smooth specimen surfaces for microscopic observation were prepared by using SiC papers and diamond pastes down to 1 μm grain size. For quantitative analysis, 20 kV acceleration voltage was applied for 50 s, and a cobalt standard was used for calibration. Inca Energy (Oxford Instruments, Analytical Ltd., Bucks, U.K.) software package was employed to process X-ray spectra.

In order to determine the crystal structures and calculate lattice parameters, X-ray diffraction analysis (XRD) was performed on powdered samples by using X'Pert MPD (Philips, Almelo, The Netherlands) vertical diffractometer. Obtained diffraction data were indexed by comparison with literature or calculated data (Powder Cell software[50]). Lattice parameters of the phases were calculated using LATCON software [51].

Vickers hardness was measured with a Reicherter instrument, with 20 Kg indentation charge. All hardness data are the average values of three experimental measurements.

2.3 Differential thermal analysis

Differential thermal analysis (DTA) was used to establish the phase transition temperature for each alloy under investigation, focusing on the ternary eutectic temperature corresponding to the so-called eutectic temperature depression. DTA was performed both on heating - to study the as cast alloys without the undercooling effect typical of aluminum alloys - and cooling. We used a Netzsch 404 C mod. Pegasus instrument, equipped with a model TASC 414/4 temperature controller. The measurements were carried out in open alumina crucibles, under a 30 mL/min Argon flux, at 5 K/min temperature rate. In the considered range, temperature accuracy was estimated to be within 0.5% of the measured value. The thermocouples were calibrated by using high purity elements such as Al, Ag, and Au as calibration materials. Melting temperature and transformation temperature points were obtained from the DTA curves using extrapolated onset temperatures, given by the intersection with the extrapolated baseline of the tangent drawn at the point of greatest slope on the leading edge of the peak.

2.4 Corrosion measurements

Corrosion behavior due to the addition of La, Pr, Sm or Tb to the Al-Si alloy was studied. The inhibiting properties of the different RE, added to the Al-Si alloy, were assessed by DC polarization potentiodynamic measurements. Curves were obtained using a Metrohm Autolab PGStat 30 potentiostat, controlled by Metrohm GPES software. These tests were carried out with 250μV/s scanning rate on specimens previously free corroded for 2, 72 and 168 hours. A three-electrode cell was used consisting of an abraded sample (down to 800 grit by SiC emery paper, suitably prepared) with an about 1 cm^2 area (working electrode), Pt spring (counter electrode), and standard calomel electrode (SCE, reference electrode) combined with a fine Lugging capillary. The corrosive solution was an aqueous 3.5 wt.% NaCl solution, pH=5.8 and D.O. (Dissolved Oxygen) = 6.5 ppm. All the experiments were conducted at room temperature (25 °C), P=1 atm and in unstirred conditions.

The working electrode consisted of an alloy incorporated into an epoxy resin with stable electric contact, in order to have a flat and regular surface. Electrochemical parameters were calculated from polarization curves. With regard to free corrosion potential (open circuit potential) and starting from -0.50 V (SCE), the working electrode potential,Efc, was increased. To calculate the corrosion current density (I*corr*) by following the Stern and Geary method [52],. a domain was selected of about -/+25 mV around Efc with a linear log I vs. E relationship Passive film breakdown potential (critical pitting potential) (Ep) and pitting protection potential (Epp) were also measured. For this purpose, the working electrode potential was again increased up to Ep value, indicated by a sharp anodic current increase. When Ep was established, the working electrode potential was decreased until the backward curve crossed the forward curve. The difference between Efc and Ep was named Pd (passivity domain), while the difference between Efc and Epp was defined as perfect passivity domain, (PPd).

Al-Si-RE alloys were also exposed to free corrosion for a period of 168 h, using the same experimental conditions as in the electrochemical tests. In order to characterize the corrosion layer and investigate surface film morphology by SEM with EDX probe, the samples, with an exposed area sometimes less than 1 cm^2, were held by a corner with a small rubber ring. and dipped in 3.5 wt.% NaCl solution . The chemical composition of the compounds in the surface first micron layer was identified by SEM-BSE (back-scattered electrons) acquisition mode.

3. Results and discussion

3.1 Microstructure, crystallography, and hardness of samples

EDX analysis of the sample microstructure (Figure 1) indicates that all the samples are made up of three phases: primary dendrites of (Al) surrounded by a ternary eutectic made up of (Al) + (Si) + Al_2Si_2RE. In all Al-Si-RE systems, the Al_2Si_2RE compound is formed and crystallizes into a hexagonal hP5-$CaLa_2O_2$ type crystal structure. The phases of the samples were confirmed by XRD analysis. Analytical results both for phase composition and lattice parameters are reported in Table 1. Figure 2 shows the XRD pattern of the Al-Si-La sample as an example: the peaks of the three phases are evident.

Although hardness is decreased by the addition of 1 wt. % RE to the Al-Si alloy, no regular trend can be identified from these initial measurements on going from La to Er in the RE series (see Table 1).

3.2 Thermal behavior

DTA measurement results, both on heating and cooling, are reported in Table 2. Thermal analyses were carried out under the same conditions for all the considered samples, with a 5 °C/min heating and cooling rate. Figure 3 shows DTA cooling curves, for three selected samples, as an example. Temperature values in Table 2 refer to primary (Al) crystallization and ternary eutectic transformation ($L \leftrightarrows Al + Si + Al_2Si_2RE$), a reaction deeply studied in the Al-Si-Sm system by [53].

When a 1 wt. %, concentration of RE is added, a ternary eutectic transformation takes place and eutectic temperature is slightly depressed. Eutectic temperature decreases by maximum four degrees if measured on heating, and from two to seven degrees if measured on cooling. The most relevant finding of these measurements is that eutectic temperature decrease seems independent of any specific RE added. There is no appreciable difference and trend in eutectic temperature lowering between the different RE elements. In the studied concentration range, the phases that have formed are (Al), (Si), and the ternary compound Al_2Si_2RE that crystallizes into all the studied ternary Al-Si-RE systems.

Figure 4 shows the micrographic appearance of Er-Al-Si samples after DTA analysis with (Al) primary crystals and the ternary eutectic (Al + Si + Al_2Si_2RE).

3.3 Corrosion behavior

Table 3 shows the electrochemical parameters obtained by polarization potentiodynamic curves for the Al-Si-RE alloys after different exposure times in 3.5 wt.% NaCl solution (Figure 5). These data show that I*corr* of the Al-Si alloys containing RE is always lower than I*corr* of the Al-Si alloy, except for the 2h exposure time. This behavior can be related to passive film formation inhibiting the corrosion process.

As a rule, the passivation film protective power can be evaluated by its inhibitory power (I%), using I*corr* obtained from electrochemical tests [54].

Inhibitory power (I%), present in Table 3, was calculated with the following equation:

$$\frac{\mathrm{I}corrAlSi \; - \; \mathrm{I}corrAlSiRE}{\mathrm{I}corrAlSi} * 100 = I\%$$

where I*corrAlSi* and I*corrAlSiRE* are the corrosion current density of the Al-Si alloys without and with RE addition, respectively. A negative or low inhibitory power after a 2h exposure would thus suggest that the surface film had not completely formed, so it cannot protect the substrate. With increasing exposure time, the inhibitory power increases. This indicates that the surface film is more protective, revealing the contribution from different RE in the passive layer. Pitting susceptibility measurements (Table 3) show that the passivity domain (Pd) and the perfect passivity domain (PPd) of all the Al-Si alloys containing RE increase in comparison with Al-Si alloy. No significant change is visible after a 2h exposure: perhaps, no consistent surface layer can be formed in such a short time. This behavior may be due to the formation of a passive film on the corroded surface, highly affected by RE presence in the substrate. High Pd and PPd are shown for Al-Si-Pr and Al-Si-Tb specimens, also due to a noticeable decrease in free corrosion potential (Efc). In general, Pd and PPd may be correlated to protective power and protection against defects of the passive film formed on the specimen surface. As shown in Table 3, Pd and PPd domains are practically non existent for the Al-Si alloy. This confirms that RE presence can significantly modify the substrate corrosion behavior. For Al-Si-Pr and Al-Si-Tb samples, a slight reduction in Pd and PPd for longer exposure time is observed. This behavior could be related to an initial decline in passive film protective power. This degradation is probably due to the long contact period between the substrate and the highly aggressive solution, containing Cl^- ions, likely to lead, for longer exposure times, to localized corrosion attacks.

Figure 6 shows SEM-BSE images of the analyzed samples. Only for Al-Si alloy, a deep localized attack can be observed. This form of corrosion is not present in the Al-Si-RE alloys exposed samples. All samples, due to their small exposure area , show a similar surface morphology. The Al-Si alloy sample (Figure 5a) reveals two separate zones, one partially oxidized, rich in Al and Si elements with, sometimes, localized corrosion attacks. The other one, slightly darker in colour, is mainly composed of aluminium oxidation products.

Conversely, all the Al-Si-RE alloy samples show three different areas, without any significant localized corrosion attack (Figure 6 b, c, d, e). In Table 4, EDX analysis results are reported for the different Al-Si-RE samples. From these results it is interesting to note:

- a clearer interphase shape area, containing a high amount of RE elements, the Al_2Si_2RE compound;
- another quite 'clear', partially oxidized zone, containing mainly Al, O, and Si;
- a third, slightly darker in colour, area, where the oxide film has homogeneously formed, in which mainly O, Al, with Cl, Na and Si traces, are present.

In these last two areas, no significant RE presence was found.

These differences in the surface layer are probably due to the small specimen size and to the rubber ring which was holding the different samples, in a significantly invasive way.

4. Conclusions

Microstructural, thermal, and corrosion effects of direct individual RE addition to a hypoeutectic Al-Si alloy in as cast condition were investigated.

EDX, and XRD analyses showed that all the samples obtained by direct La, Pr, Nd, Sm, Gd, Tb, Dy, or Er addition to the Al-Si alloy consisted of three phases: primary dendrites of (Al) surrounded by the ternary eutectic made up of (Al) + (Si) + Al_2Si_2RE. Vickers hardness measurements pointed to decreased hardness, but no regular trend could be observed in such decrease on going from La to Er.

Eutectic temperature decrease due to RE addition was evident, and similar for all considered RE. Such decrease can be useful in the industrial field to control alloy structure changes induced by RE in the as cast alloys. For this purpose, is more interesting to investigate the heating curves.

No in-depth investigations have been found in the literature on the effects on corrosion behavior of Al-Si Alloy with directly added RE as a further alloying metal. In this paper, corrosion behavior due to the addition of La, Pr, Sm or Tb to an Al-Si alloy was studied in 3.5 wt.% NaCl solution. After a 2h exposure, a homogeneous surface layer was not completely formed, and it was not able to protect the substrate. With increasing exposure time, the presence of a passive film on Al-Si-RE alloys was proved. This layer had protective characteristics and revealed the contribution of the

different RE. As expected due to experimental conditions, the layer morphology was complex. If transferred to industrial field, direct RE direct addition to Al-Si alloys could reduce or eliminate the pre-treatment processes before the application of the primer and top coat on the substrate, thus offering a significant advantage in terms of manufacturing time and costs.

Acknowledgements.

Carlo Bottino is gratefully acknowledged for his technical support. This work has been funded by the Italian Ministry of University and Research in the framework of the RITMARE Flagship Project.

References

[1] B.E. Slattery, T. Perry, A. Edrisy, Microstructural evolution of a eutectic Al-Si engine subjected to severe running conditions, Mat. Sci. Eng. A 512 (2009) 76-81.

[2] W.S. Miller, L. Zhuang, J. Bottema, A.J. Wittebrood, P. De Smet, A. Haszler, A. Vieregge, Recent development in aluminium alloys for the automotive industry, Mat. Sci. Eng. A 280 (2000) 37-49.

[3] M. Zhu, Z. Jian, L. Yao, C. Liu, G. Yang, Y. Zhou Y, Effect of mischmetal modification treatment on the microstructure, tensile properties, and fracture behavior of Al-7.0%Si-0.3%Mg foundry aluminum alloys, J. Mater. Sci. 46 (2011) 2685-2694.

[4] A. Mazahery, M.O. Shabani, Modification Mechanism and Microstructural Characteristics of Eutectic Si in Casting Al-Si Alloys: A Review on Experimental and Numerical Studies, Jom-J. Min. Met. Mat. S., l66 (5) (2014) 726-738.

[5] P. Traverso, R. Spiniello, L. Monaco, Corrosion Inhibition of Al 6061T6/Al_2O_3p 10% (v/v) composite in 3.5% NaCl solution with addition of cerium (III) chloride, Surf. Interface Anal. 34 (2002) 185-188.

[6] J. Li, B. Hurley, R. Buchheit, Microelectrochemical Characterization of the Effect of Rare Earth Inhibitors on the Localized Corrosion of AA2024-T3, J. Electrochem. Soc. 162 (10) (2015) C563-C571.

[7] M. Kendig, S. Jeanjaquet, R. Addison, J. Waldrop, Role of hexavalent chromium in the inhibition of corrosion of aluminium alloys, Surf. Coat. Tech. 140 (2001) 58-66.

[8] J. Zhao, L. Xia, A. Sehgal, D. Lu, R.L. McCreery, G.S. Frankel, Effects of chromate and chromate conversion coatings on corrosion of aluminium alloy 2024-T3, Surf. Coat. Tech. 140 (2001) 51-57.

[9] O. Lunder, J.C.Walmsley, P. Mack, K. Nisancioglu, Formation and characterization of a chromate conversion coating on AA6060 aluminium, Corros. Sci. 47 (2005) 1604-1624.

[10] A. Bahadur, Chromates as Corrosion Inhibitors for Aqueous Systems, Corros. Rev. 10 (1-2) (1992) 155-178.

[11] Agency for Toxic Substances and Disease Registry (ATSDR). Toxicological Profile for Chromium. ATSDR/TP-88/10. U.S. Department of Health and Human Services. Atlanta, Georgia: U.S. Public Health Service, 1989.

[12] R. Garton, Biological Effects of Cooling Tower Blowdown, NERC, Corvallis, 1987.

[13] A.K. Mishra, R. Balasubramaniam, Corrosion inhibition of aluminum alloy AA 2014 by rare earth chlorides, Corros. Sci. 49 (2007) 1027-1044.

[14] E.A. Matter, S. Kozhukharov, M. Machkova, V. Kozhukharov, Comparison between the inhibition efficiencies of Ce(III) and Ce(IV) ammonium nitrates against corrosion of AA2024 aluminum alloy in solutions of low chloride concentration, Corros. Sci. 62 (2012) 22-33.

[15] T. Behrsing, G.B. Deacon, P.C. Junk, The chemistry of rare earth metals, compounds, and corrosion inhibitors. Ch 1 of Rare earth based corrosion inhibitors, M. Forsyth and B. Hinton (eds.), Elsevier, UK, 2014.

[16] B. Gu, J. Liu, Corrosion Inhibition Mechanism of Rare Earth Metal on LC4 Al Alloy with Split Cell Technique, J. Rare Earth. 24 (2006) 89–96.

[17] J. Hill, T. Markleya, M. Forsytha, P.C. Howletta, B.R.W. Hinton, Corrosion inhibition of 7000 series aluminium alloys with cerium diphenyl phosphate, J. Alloy. Compd. 509 (2011) 1683-1690.

[18] Y. Liu, Y.F. Cheng, Inhibiting effect of cerium ions on corrosion of 3003 aluminum alloy in ethylene glycol–water solutions, J. Appl. Electrochem. 41 (2011) 383-388.

[19] M. Forsyth, M. Seter, B. Hinton, G. Deacon, P. Junk, New 'Green' Corrosion Inhibitors Based on Rare Earth Compounds, Aust. J. Chem. 64 (2011) 812-819.

[20] E.A. Matter, S. Kozhukharov, M. Machkova, V. Kozhukharov, Electrochemical studies on the corrosion inhibition of AA2024 aluminium alloy by rare earth ammonium nitrates in 3.5% NaCl solutions, Mater. Corros. 64 (2013) 408-414.

[21] M. Bethencourt, F.J. Botana, M.A. Cauqui, M. Marcos, M.A. Rodrìguez, J.M. Rodrìguez Izquierdo, Protection against corrosion in marine environments of AA5083 Al–Mg alloy by lanthanide chlorides, J. Alloy. Compd. 250 (1997) 455–460.

[22] A.J. Aldykewicz, H.S. Isaacs, A.J. Davenport, Investigation of cerium as a cathodic inhibitor for aluminium–copper alloys, J. Electrochem. Soc. 142 (1995) 3342.

[23] A. Aballe, M. Bethencourt, F.J. Botana, M.J. Cano, M. Marcos, Inhibition of the corrosion process of alloy AA5083 in seawater by cerium cations. An EIS study, Mater. Corros. 52 (2001) 344–350.

[24] K.A. Yasakau, M.L. Zheludkevich, S.V Lamaka, M.G.S. Ferreira, Mechanism of Corrosion Inhibition of AA2024 by Rare-Earth Compounds, J. Phys. Chem. B 110 (2006) 5515-5528.

[25] B. Li, Q.L. Pan, Z.Y. Zhang, C. Li, Characterization of flow behavior and microstructural evolution of Al–Zn–Mg–Sc–Zr alloy using processing maps, Mat. Sci. Eng. A 556 (2012) 844-848.

[26] B. Li, Q.L. Pan, Z.Y. Zhang, C. Li, Research on intercrystalline corrosion, exfoliation corrosion, and stress corrosion cracking of Al–Zn–Mg–Sc–Zr alloy, Mater. Corros. 64 (2013) 592-598.

[27] L.M. Wu, M. Seyring, M. Rettenmayr, W.H. Wang, Characterization of precipitate evolution in an artificially aged Al–Zn–Mg–Sc–Zr alloy, Mat. Sci. Eng. A 527 (2010) 1068-1073.

[28] L.M. Wu, W.H. Wang, Y.F. Hsu, S. Trong, Effects of homogenization treatment on recrystallization behavior and dispersoid distribution in an Al–Zn–Mg–Sc–Zr alloy, J. Alloy. Compd. 456 (2008) 163-169.

[29] Y. Deng, Z.M. Yin, J.Q. Duan, K. Zhao, B. Tang, Z.B. He, Evolution of microstructure and properties in a new type 2 mm Al–Zn–Mg–Sc–Zr alloy sheet, J. Alloy. Compd. 517 (2012) 118-126.

[30] X. Huang, Q. Pan, B. Li, Z. Liu, Z. Huang, Z. Yin, Microstructure, mechanical properties and stress corrosion cracking of Al-Zn-Mg-Zr alloy sheet with trace amount of Sc, J. Alloy. Compd. 650 (2015) 805-820.

[31] R.K.R. Singh, C. Sharma, D.K. Dwivedi, N.K. Mehta, P. Kumar, The microstructure and mechanical properties of friction stir welded Al–Zn–Mg alloy in as welded and heat treated conditions, Mater. Design. 32 (2011) 682-687.

[32] K.E. Knipling, D.N. Seidman, D.C. Dunand, Ambient- and high-temperature mechanical properties of isochronally aged Al–0.06Sc, Al–0.06Zr and Al–0.06Sc–0.06Zr (at.%) alloys, Acta Mater. 59 (2011) 943-954.

[33] S.P.Wen, K.Y. Gao,Y. Li, H. Huang, Z.R. Nie, Synergetic effect of Er and Zr on the precipitation hardening of Al–Er–Zr alloy, Scripta Mater. 65 (2011) 592-595.

[34] A. Heinz, A. Haszler, C. Keidel, S. Moldenhauer, R. Benedictus, W.S. Miller, Recent development in aluminium alloys for aerospace applications, Mat. Sci. Eng., A 280 (2000) 102-107.

[35] Z. Ahmad, A. Ul-Hamid, B.J. Abdul-Alim, The corrosion behavior of scandium alloyed Al 5052 in neutral sodium chloride solution, Corros. Sci. 43 (2001) 1227-1243.

[36] M.K. Cavanaugh, N. Birbilis, R.G. Buchheit, F. Bovard, Investigating localized corrosion susceptibility arising from Sc containing intermetallic Al3Sc in high strength Al-alloys, Scripta Mater. 56 (2007) 995-998.

[37] B. Li, Q. Pan, X. Huang, Z. Yin, Microstructures and properties of Al–Zn–Mg–Mn alloy with trace amounts of Sc and Zr, Mat. Sci. Eng. A 616 (2014) 219-228.

[38] J.S. Vetrano, S.M. Bruemmer, L.M. Pawlowski, I.M. Robertson, Influence of the particle size on recrystallization and grain growth in Al-Mg-X alloys, Mat. Sci. Eng., A 238 (1997) 101-107.

[39] V.G. Davydov, T.D. Rostova, V.V. Zakharov, Y.A. Filatov, V.I. Yelagin, Scientific principles of making an alloying addition of scandium to aluminium alloys, Mat.. Sci. Eng. A 280 (2000) 30-36.

[40] S. Komura, Z. Horita, M. Furukawa, M. Nemoto, T.G. Langdon, Influence of scandium on superplastic ductilities in an Al–Mg–Sc alloy, J. Mater. Res. 15 (2000) 2571-2576.

[41] F. Rosalbino, E. Angelini, S. De Negri, A. Saccone, S. Delfino, Influence of the rare earth content on the electrochemical behaviour of Al–Mg–Er alloys, Intermetallics 11 (2003) 435-441.

[42] H.C. Fang, K.H. Chen, X. Chen, H. Chao, G.S. Peng, Effect of Cr, Yb and Zr additions on localized corrosion of Al–Zn–Mg–Cu alloy, Corros. Sci. 51 (2009) 2872-2877.

[43] Y. Wang, R.K. Gupta, N.L. Sukiman, R. Zhang, C.H.J. Davies, N. Birbilis, Influence of alloyed Nd content on the corrosion of an Al–5Mg alloy, Corros. Sci. 73 (2013) 181-187.

[44] H.C. Fang, K.H. Chen, X. Chen, L.P. Huang, G.S. Peng, B.Y. Huang, Effect of Zr, Cr and Pr additions on microstructures and properties of ultra-high strength Al–Zn–Mg–Cu alloys, Mat. Sci. Eng. A 528 (2011) 7606-7615.

[45] H.C. Fang, H.Chao, K.H.Chen, Effect of Zr, Er and Cr additions on microstructures and properties of Al–Zn–Mg–Cu alloys, Mat. Sci. Eng. A 610 (2014) 10-16.

[46] L. Heusler, W. Schneider, Influence of alloying elements on the thermal analysis results of Al-Si cast alloys, Journal of Light Metals, 2 (2002) 17-26.

[47] H. Qiu, H. Yan, Z. Hu, Modification of near-eutectic Al–Si alloys with rare earth element samarium, J. Mater. Res. 29 (2014) 1270-1277.

[48] K. Nogita, H. Yasuda, M. Yoshiya, S.D. Mc.Donald, K. Uesugi, A. Tacheuchi, Y. Suzuki, The role of trace element segregation in the eutectic modification of hypoeutectic Al-Si alloys, J. Alloy. Compd. 489 (2010) 415-420.

[49] A.M. Cardinale, D. Macciò, S. Delfino, A. Saccone, Phase equilibria of the Dy-Al-Si system at 500°C, J. Therm. Anal. Calorim. 103 (2012) 103-109.

[50] W. Kraus, G. Nolze, Powder Cell for Windows, Berlin (1999).

[51] G. King, D. Schwarzenbach Latcon, Xtal3.7 System, in: S.R. Hall, D.J. du Boilay, R. Olthof-Hazekamp (Eds), University of Western, Australia, 2000.

[52] M. Stern, A.L. Geary, Electrochemical Polarization: A Theoretical Analysis of the Shape of Polarization Curves, J. Electrochem. Soc. 104 (1957) 56-63.

[53] B. Markoli, S. Spaic, F. Zupanic, The constitution of alloys in the Al-rich corner of the Al-Si-Sm ternary system, Z. Metallkd. 92 (2001) 1098-1102.

[54] A.M. Beccaria, G. Padelletti, G. Montesperelli, L. Chiaruttini, The effect of pretreatments with siloxanes on the corrosion resistance of aluminium in NaCl solution, Surf. Coat. Tech. 11 (1999) 240-246.

Table 1. Gross composition, phase analysis and Vickers hardness of the Al-Si-RE alloys.

Al-Si Alloy	Nominal composition (wt. %)	Phase analysis and crystal structure XRD results	EDX results (wt. %)	Lattice parameters (nm)		Vickers hardness ($Kgmm^{-2}$)
	Al, Si, RE		Al, Si, RE	a	c	
Al-Si	88.5, 11.5, 0.0	(Al) *cF4-Cu*	98.4, 1.6, 0.0			74.5
		(Si) *cF8 C(diamond)*	0.0, 100.0, 0.0			
Al-Si-La	87.0, 12.0, 1.0	(Al) *cF4-Cu*	99.0, 1.0, 0.0	0.4048(1)		44.0
		(Si) *cF8 C(diamond)*	7.0, 93.0, 0.0	0.5429(1)		
		$LaAl_2Si_2$ *hP5-*$CaLa_2O_2$	20.0, 22.5, 57.5	0.4225(3)	0.6985(3)	
Al-Si-Pr	91.0, 8.0, 1.0	(Al) *cF4-Cu*	99.0, 1.0, 0.0	0.4050(1)		44.0
		(Si) *cF8 C (diamond)*	2.5, 97.5, 0.0	0.5430(1)		
		$PrAl_2Si_2$ *hP5-*$CaLa_2O_2$	20.0, 23.0, 57.0	0.4219(4)	0.6873(3)	
Al-Si-Nd	90.0, 9.0, 1.0	(Al) cF4-Cu	90.0, 10.0, 0.0	0.4050(1)		56.0
		(Si) *cF8 C(diamond)*	1.5, 98.5, 0.0	0.5430(2)		
		$NdAl_2Si_2$ *hP5-*$CaLa_2O_2$	*	0.4231(0)	0.6747(3)	
Al-Si-Sm	88.0, 11.0, 1.0	(Al) cF4-Cu	98.5, 1.5, 0.0	0.4054(2)		49.0
		(Si) *cF8 C (diamond)*	1.0, 99.0, 0.0	0.5438(1)		
		$SmAl_2Si_2$ *hP5-*$CaLa_2O_2$	19.5, 21.5, 59.0	0.4190(5)	0.6716(5)	
Al-Si-Gd	88.5, 10.0, 1.5	(Al) cF4-Cu	97.5, 2.5, 0.0	0.40483)		67.5
		(Si) *cF8 C (diamond)*	1.5, 98.5, 0.0	0.5423(1)		
		$GdAl_2Si_2$ *hP5-*$CaLa_2O_2$	*	0.4172(6)	0.6638(3)	
Al-Si-Tb	87.5, 11.0, 1.5	(Al) *cF4-Cu*	98.5, 1.5, 0.0	0.4053(1)		58.0
		(Si) *cF8 C (diamond)*	5.0, 95.0, 0.0	0.5430(3)		
		$TbAl_2Si_2$ *hP5-*$CaLa_2O_2$	20.0, 20.0, 60.0	0.4184(4)	0.6605(4)	
Al-Si-Dy	88.5, 10.0, 1.5	(Al) *cF4-Cu*	98.0, 2.0, 0.0	0.4057(0)		65.0
		(Si) *cF8 C (diamond)*	2.0, 98.0, 0.0	0.5437(1)		
		$DyAl_2Si_2$ *hP5-*$CaLa_2O_2$	20.0, 22.0, 58.0	0.4187(3)	0.6567(1)	
Al-Si-Er	87.5, 11.5, 1.0	(Al) cF4-Cu	98.0, 2.0, 0.0	0.4049(1)		46.0
		(Si) *cF8 C (diamond)*	0.0, 100.0, 0.0	0.5428(3)		
		$ErAl_2Si_2$ *hP5-*$CaLa_2O_2$	*	0.4175(2)	0.6479(4)	

*crystals too small to be analyzed by means of EDX

Table 2. Thermal effect measured by DTA (on heating and on cooling) on the Al-Si-RE alloys.

Alloy	**Differential thermal analysis results (°C)**			
	heating		**cooling**	
	(Al)	**Eutectic**	**(Al)**	**Eutectic**
Al-Si	597	580	596	575
Al-Si-La	601	580	604	568
Al-Si-Pr	595	579	600	572
Al-Si-Nd	595	580	612	575
Al-Si-Sm	605	578	605	572
Al-Si-Gd	606	578	606	573
Al-Si-Tb	610	577	604	570
Al-Si-Dy	603	577	602	573
Al-Si-Er	597	576	599	567

Table 3. Electrochemical parameters obtained by polarization potentiodynamic curves of different Al-Si-RE alloys, after different exposure times in 3.5 wt.% NaCl solution.

Alloy	**Exposure time (h)**	**I corr ($\mu A\ cm^{-2}$)**	**E fc (mV)**	**E p (mV)**	**E pp (mV)**	**P d (mV)**	**PP d (mV)**	**I (%)**
Al-Si	2	0,21	-750	-----	-----	-----	-----	----
	72	0,35	-745	-728	-745	17	0	----
	168	0.80	-750	-----	-----	-----	-----	----
Al-Si-La	2	0.07	-740	-----	-----	-----	-----	67
	72	0.15	-780	-704	-740	76	40	57
	168	0.09	-795	-718	-728	77	67	89
Al-Si-Pr	2	0.41	-737	-----	-----	-----	-----	-95
	72	0.18	-950	-700	-775	250	175	49
	168	0.14	-930	-720	-782	210	148	83
Al-Si-Sm	2	0.26	-733	-----	-----	-----	-----	-24
	72	0.17	-850	-710	-758	140	92	52
	168	0.25	-860	-718	-783	142	77	69
Al-Si-Tb	2	0.20	-741	-----	-----	-----	-----	5
	72	0.20	-990	-725	-760	265	230	43
	168	0.08	-930	-730	-777	200	153	90

Reference Electrode: SCE (Standard Calomel Electrode)

Table 4. EDX analysis results for the different Al-Si-RE alloys, after 168 h exposure time in 3.5 wt.% NaCl solution.

Alloy	Point of analysis	EDX analysis results (wt. %)					
		O	Al	Si	Na	Cl	R
Al-Si	1	18,3	68,7	12,1	0,6	0,3	-----
	2	57,1	35,2	1,2	3,9	2,6	-----
Al-Si-La	1	6,7	13,2	10,6	0,9	0,3	68,3
	2	20,8	62,1	14,3	1,8	1,0	0,0
	3	59,0	33,0	1,0	2,1	4,9	0,0
Al-Si-Pr	1	9.7	15,3	27,7	0,0	0,2	47,1
	2	45,2	51,6	2,9	0,2	0,3	0,0
	3	68,0	32,0	0.0	0,0	0,0	0,0
Al-Si-Sm	1	13,3	19,3	18,0	0,1	0,3	49,0
	2	27,1	70,3	2,2	0,2	0,2	0,0
	3	59,5	36,5	1,3	1,7	1,0	0,0
Al-Si-Tb	1	6,2	22,8	23,2	0,0	0,0	47,8
	2	17,8	80,1	1,7	0,2	0,2	0,0
	3	64,3	31,6	0,5	1,0	2,6	0,0

Figure captions

Figure 1: SEM-BSE images: a) Al-Si-La, b) Al-Si-Pr, c) Al-Si-Nd, d) Al-Si-Sm, e) Al-Si-Gd, f) Al-Si-Tb, g) Al-Si-Dy, and h) Al-Si-Er alloy samples. Each sample is constituted by primary black (Al) crystals surrounded by the ternary eutectic decomposition: (Al) + (Si) + Al_2Si_2RE.

Figure 2: XRD pattern of the Al-Si-La alloy (Al-87 wt. % Si-12 wt. % and La-1 wt. %). From X-ray diffraction analysis the following intermetallic phases have been recognized: (Al) cF4-Cu, (Si) cF8-C_{diam} and $LaAl_2Si_2$ hP5-$CaAl_2O_2$.

Figure 3: SEM-BSE image of the Er-Al-Si alloy, after DTA analysis, showing the primary (Al) crystal surrounded by the ternary eutectic decomposition: (Al) + (Si) + Al_2Si_2Er.

Figure 4: DTA cooling curve of: a) Al-Si-La, b) Al-Si-Gd, and c) Al-Si-Er alloys.

Figure 5: Polarization potentiodynamic curves for the Al-Si-RE alloys after different exposure times (a= 2h, b=72h, c=168h) in 3.5 wt.% NaCl solution.

Figure 6: SEM-BSE images of some Al-Si-RE alloy samples, after 168 h of free exposure time in 3.5 wt.% NaCl solution. a) Al-Si, b) Al-Si-La, c) Al-Si-Pr, d) Al-Si-Sm, e) Al-Si-Tb. In each figure are marked the analysed points (see Table 4); point analysis (circles), area analysis (squares).

Highlights

- Effects of different RE addition on a hypoeutectic as cast Al-Si alloy are studied
- EDX, XRD, and DTA analyses of Al-Si-RE samples are carried out
- Decrease in eutectic temperature is similar for all Al-Si-RE samples
- Decrease in Vickers hardness is similar for all Al-Si-RE samples
- RE addition increases corrosion resistance in 3.5 wt.% NaCl solution

Figure
Click here to download high resolution image

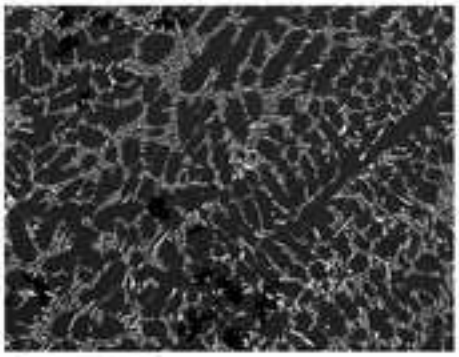

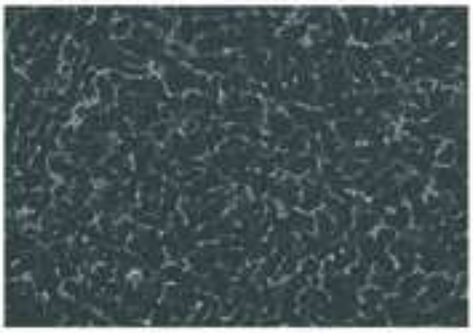

Figure

Click here to download high resolution image

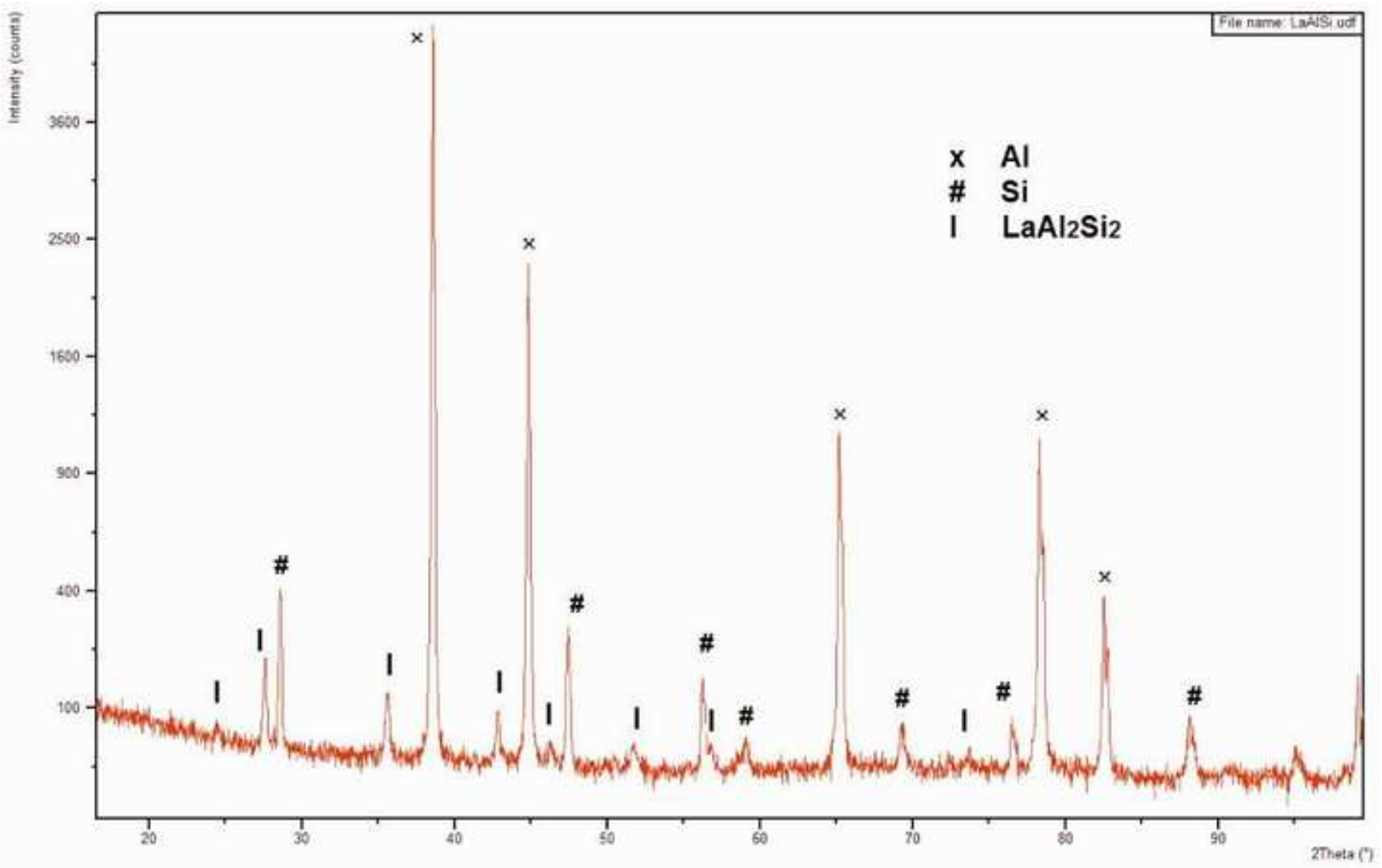

Figure

Click here to download high resolution image

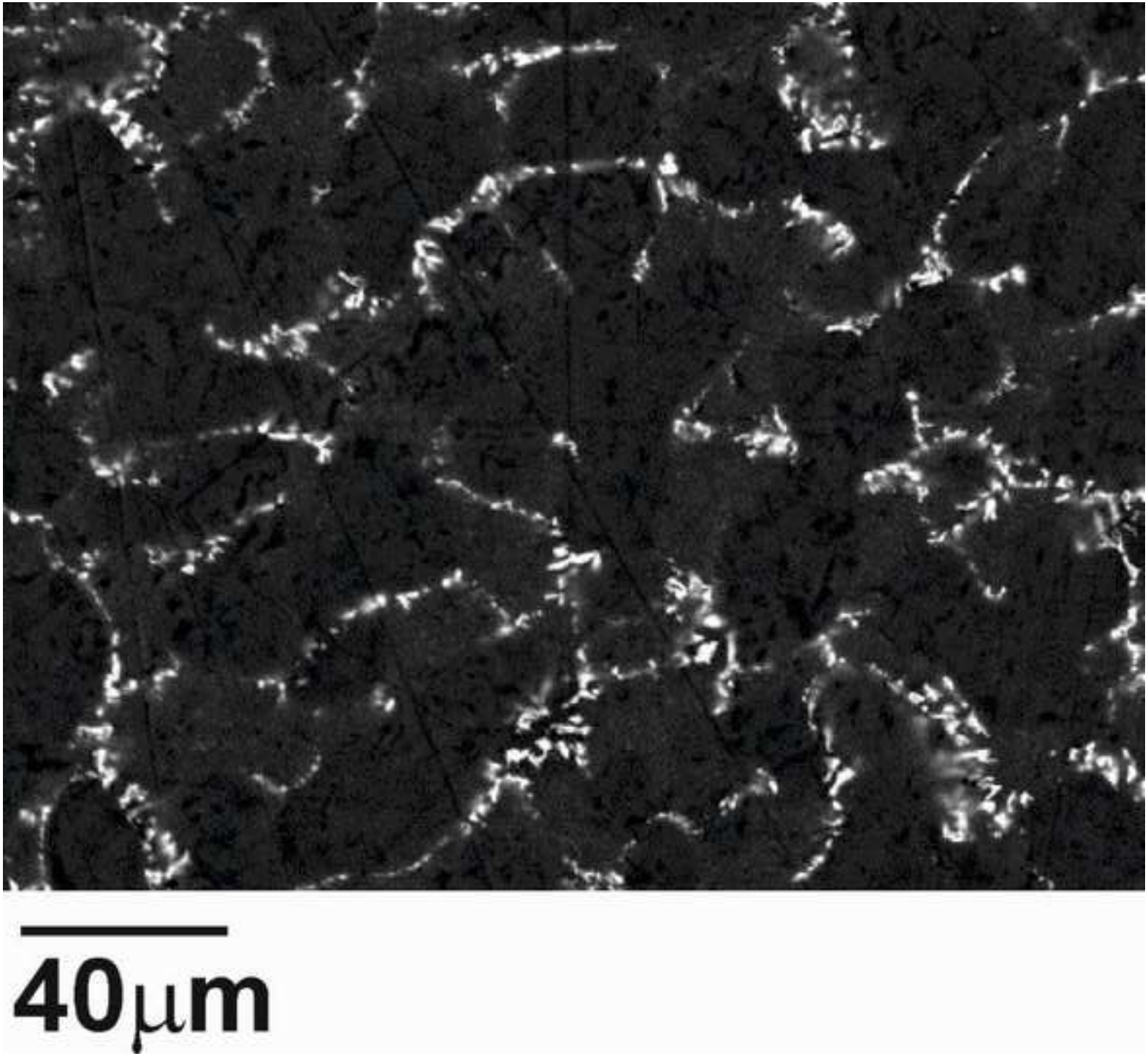

Figure

Click here to download high resolution image

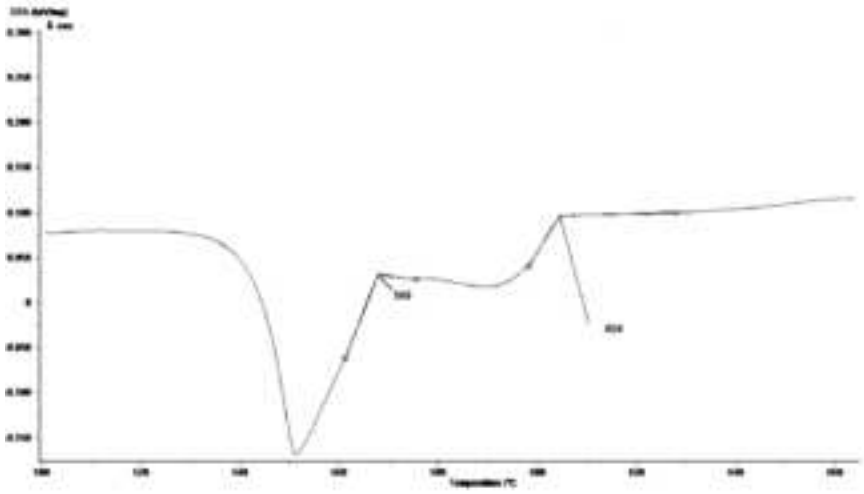

a)

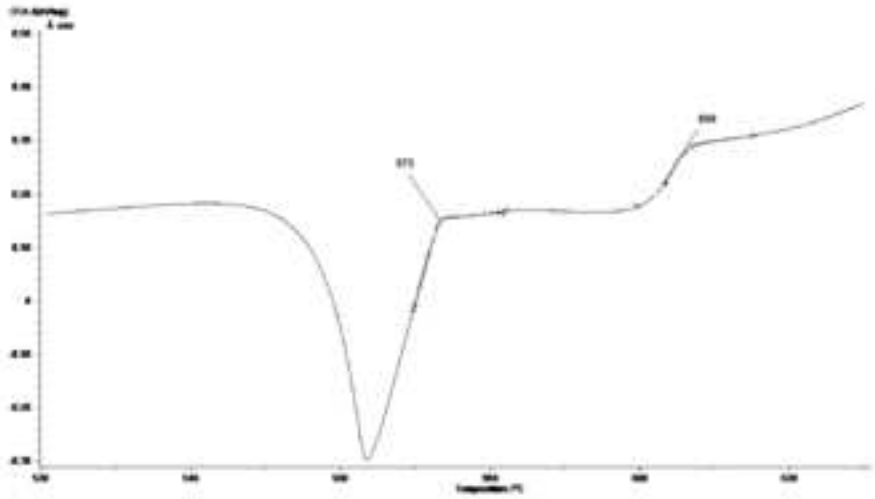

b)

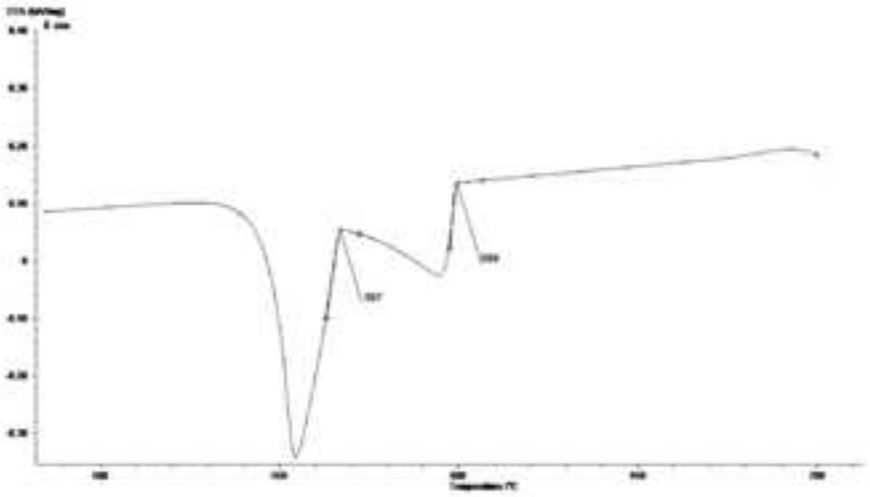

c)

Figure

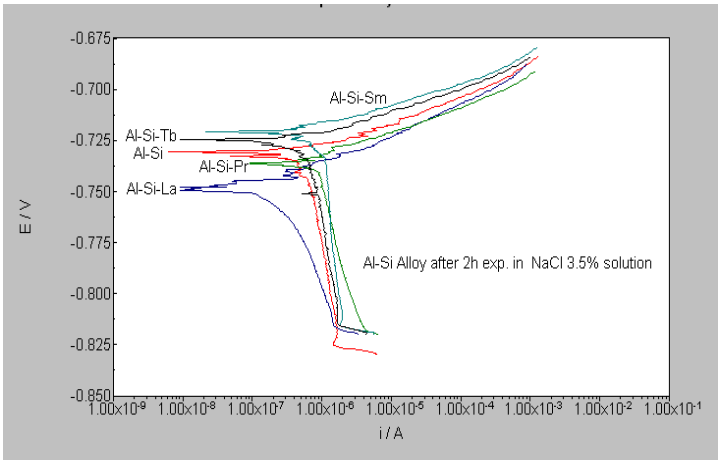
-0.675
-0.700
-0.725
-0.750
-0.775
-0.800
-0.825
-0.850
E / V
Al-Si-Sm
Al-Si-Tb
Al-Si
Al-Si-Pr
Al-Si-La
Al-Si Alloy after 2h exp. in NaCl 3.5% solution
1.00x10-9 1.00x10-8 1.00x10-7 1.00x10-6 1.00x10-5 1.00x10-4 1.00x10-3 1.00x10-2 1.00x10-1
i / A

a)

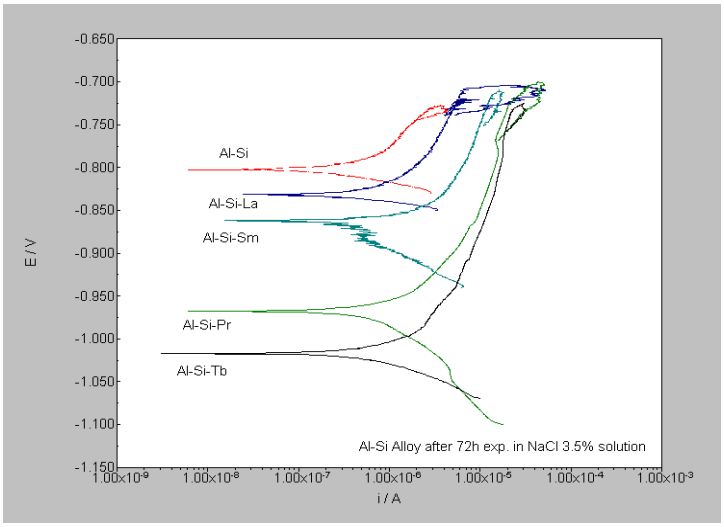
-0.650
-0.700
-0.750
-0.800
-0.850
-0.900
-0.950
-1.000
-1.050
-1.100
-1.150
E / V
Al-Si
Al-Si-La
Al-Si-Sm
Al-Si-Pr
Al-Si-Tb
Al-Si Alloy after 72h exp. in NaCl 3.5% solution
1.00x10-9 1.00x10-8 1.00x10-7 1.00x10-6 1.00x10-5 1.00x10-4 1.00x10-3
i / A

b)

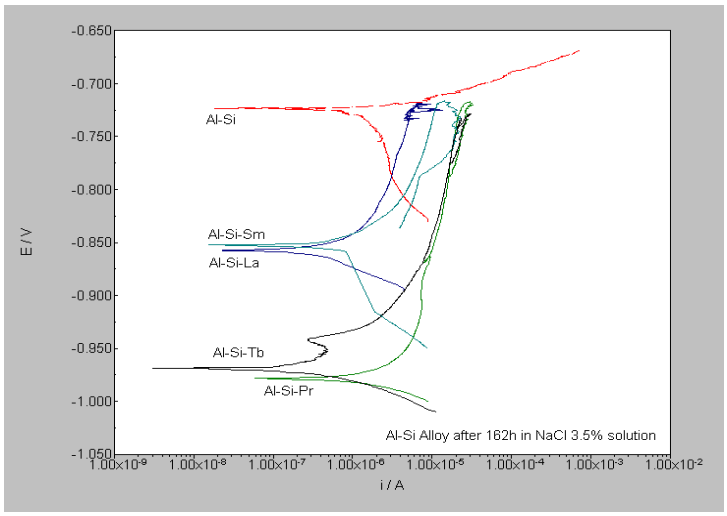
-0.650
-0.700
-0.750
-0.800
-0.850
-0.900
-0.950
-1.000
-1.050
E / V
Al-Si
Al-Si-Sm
Al-Si-La
Al-Si-Tb
Al-Si-Pr
Al-Si Alloy after 162h in NaCl 3.5% solution
1.00x10-9 1.00x10-8 1.00x10-7 1.00x10-6 1.00x10-5 1.00x10-4 1.00x10-3 1.00x10-2
i / A

c)

Figure

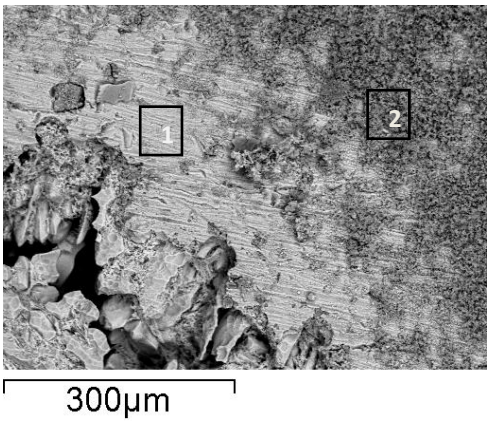

a)

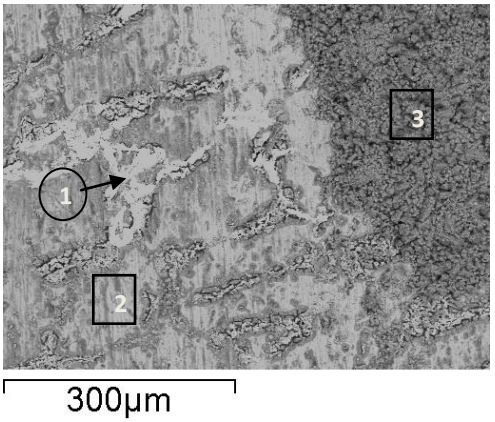

b)

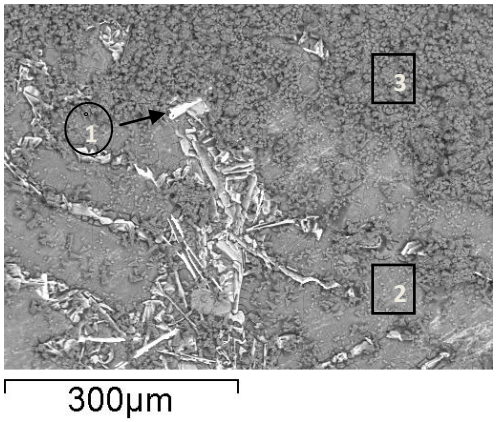

c)

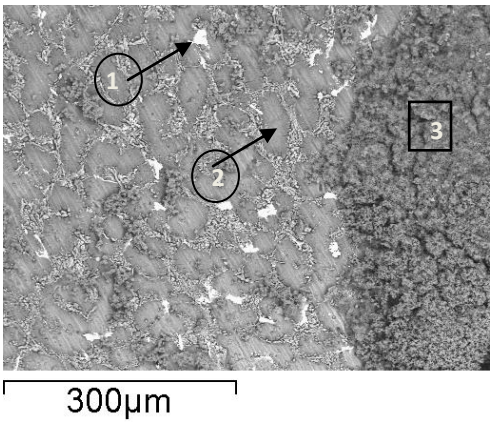

d)

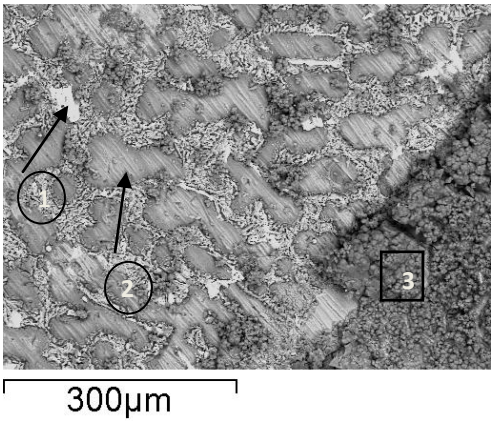

e)